
Web-Scale Collection of Video Data for 4D Animal Reconstruction

Brian Nlong Zhao^{1,2} Jiajun Wu^{1†} Shangzhe Wu^{1,3†}

¹Stanford University ²University of Illinois Urbana-Champaign ³University of Cambridge

Abstract

Computer vision for animals holds great promise for wildlife research but often depends on large-scale data, while existing collection methods rely on controlled capture setups. Recent data-driven approaches show the potential of single-view, non-invasive analysis, yet current animal video datasets are limited—offering as few as 2.4K 15-frame clips and lacking key processing for animal-centric 3D/4D tasks. We introduce an automated pipeline that mines YouTube videos and processes them into object-centric clips, along with auxiliary annotations valuable for downstream tasks like pose estimation, tracking, and 3D/4D reconstruction. Using this pipeline, we amass 30K videos (2M frames)—an order of magnitude more than prior works. To demonstrate its utility, we focus on the 4D quadruped animal reconstruction task. To support this task, we present Animal-in-Motion (AiM), a benchmark of 230 manually filtered sequences with 11K frames showcasing clean, diverse animal motions. We evaluate state-of-the-art model-based and model-free methods on Animal-in-Motion, finding that 2D metrics favor the former despite unrealistic 3D shapes, while the latter yields more natural reconstructions but scores lower—revealing a gap in current evaluation. To address this, we enhance a recent model-free approach with sequence-level optimization, establishing the first 4D animal reconstruction baseline. Together, our pipeline, benchmark, and baseline aim to advance large-scale, markerless 4D animal reconstruction and related tasks from in-the-wild videos. Code and datasets are available at <https://github.com/briannlongzhao/Animal-in-Motion>.

1 Introduction

The study of animals has long fascinated scientists across fields—from wildlife conservation to biomechanics and robotics. Traditionally, capturing visual data of animal shape and motion requires sophisticated, often expensive, marker-based systems [32, 71]. Modern computer vision techniques offer an alternative approach of purely image-based, markerless motion capture [77, 40, 19, 26]. However, many of these methods depend on multi-view images captured in controlled settings, limiting their applicability to real-world, in-the-wild animal behavior. Recent advancements in tasks such as pose estimation, tracking, and, most challengingly, 3D/4D reconstruction, have enabled efficient analysis of animals from single-view images or videos. Data-driven approaches for animal shape and motion analysis and reconstruction have shown robust performance by leveraging 3D priors, either from scanned models [74, 42, 8, 9] or from optimization over feature correspondences [61, 35, 66]. This opens the door to scalable, non-invasive capture of animal behavior using monocular images and videos collected in the wild. Similar to other areas of machine learning, the progress depends heavily on the availability of large-scale data. Yet, even the largest available animal-centric video datasets remain inadequate, as they contain only 2.4K short clips of 15 frames each, lack object-centric views, and omit crucial data needed for challenging tasks such as 4D animal reconstruction

[†]Equal advising.

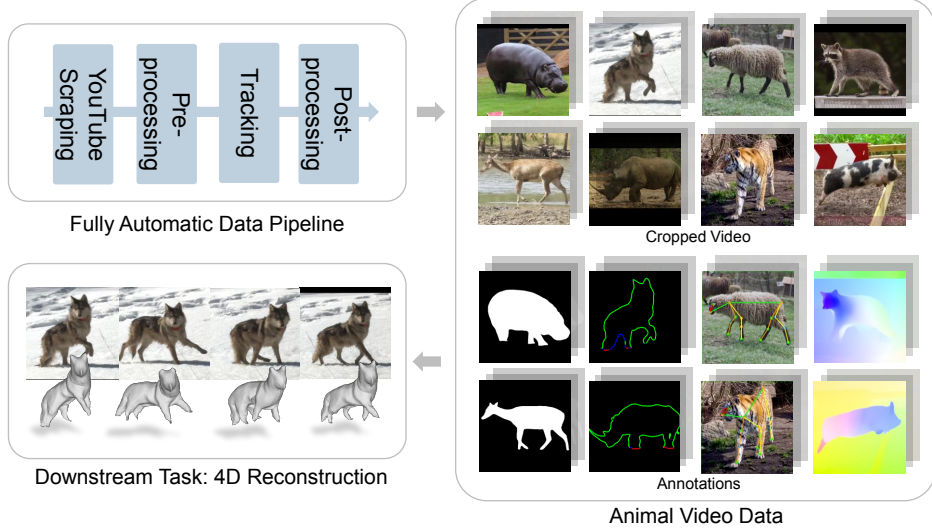


Figure 1: We propose a fully automated data pipeline to collect and process data from scratch, making it ready for downstream tasks such as 4D animal reconstruction.

[68]. The only existing dataset truly suitable for 4D animal reconstruction is even more limited, with only 11 videos in total [8].

In this paper, we introduce a scalable, automated pipeline that enables large-scale video collection and processing for animal shape and motion analysis, with a particular focus on the downstream task of 4D quadruped reconstruction. Our pipeline scrapes raw video from YouTube, exploiting its vast scale and diversity. The videos are then processed into object-centric video clips, along with additional processed features, including instance masks, keypoints, optical flow, and occlusion boundaries, all in a fully automatic manner. These features can be used to aid the downstream task of reconstructing 3D shape and motion of animals, without requiring any explicit 3D annotation. With this pipeline, we obtained an object-centric video dataset of 30K clips, consisting of 2 million frames.

Furthermore, we introduce Animal-in-Motion (AiM), the first benchmark dataset specifically designed for 4D quadruped pose and shape reconstruction. Our dataset contains 230 carefully curated animal motion sequences, totaling 11,061 frames, all collected by our proposed framework. We ensure that each selected sequence has accurate silhouettes and keypoints. We adopt metrics widely used in prior 3D animal reconstruction research. Since no existing methods explicitly target 4D animal reconstruction, we benchmark state-of-the-art 3D approaches—covering both model-based and model-free methods—by evaluating their per-frame performance on Animal-in-Motion. We find that model-based methods often achieve higher scores, yet may produce unrealistic shapes and poses, while model-free methods generate more natural and temporally coherent 3D reconstructions but score lower, revealing a mismatch between evaluation and perceptual quality. This exposes the limitations of 2D-based metrics that are commonly used by the community and underscores the importance of qualitative assessment in 3D and the need for better 3D-aware metrics.

Based on these findings, we also enhance the reconstruction quality of the model-free approach, improving its 2D metrics while retaining natural, consistent 3D poses, shapes, and motion. Specifically, we build upon 3D-Fauna [35], a model-free quadruped reconstruction method that operates in a feed-forward manner across various animal categories. To boost its performance, we incorporate additional keypoint supervision for more precise pose estimation and introduce several optimizations, including smoothness losses, that facilitate effective per-sequence refinement. Our benchmarking and qualitative assessments demonstrate that these modifications yield improvements on all quantitative metrics, while concurrently producing more natural and temporally coherent 3D shapes and motions that better resemble the input videos.

In summary, our contributions are as follows:

- We introduce a unified, automated data pipeline that can collect and process noisy YouTube videos into object-centric clips prepared for downstream tasks such as 4D animal reconstruction.

- We present Animal-in-Motion (Animal-in-Motion), the first benchmark evaluation dataset for 4D quadruped reconstruction.
- We propose 4D-Fauna, a new model-free 4D animal reconstruction baseline that adapts 3D-Fauna with extra guidance and losses to enable more accurate reconstruction on video.
- We present analyses of the benchmarking results for current model-based and model-free approaches, revealing gaps in current metrics and suggesting directions for future evaluation design.

2 Related Works

2.1 Animal Reconstruction from Image

The task of 4D animal reconstruction extends from 3D animal reconstruction, which focuses on estimating 3D pose and shape of an animal from a 2D image, and 4D reconstruction results can be obtained by applying 3D reconstruction methods independently to each video frame. Numerous studies have explored the 3D animal reconstruction task, primarily using either a model-based or model-free approach. Typical model-based approaches include ABM [4], SMAL [74], and their variations and extensions [58, 75, 76, 9, 48, 49, 31, 8, 38]. These methods start with a prior 3D mesh and optimize a set of predefined pose and deformation parameters to fit the 2D ground truth labels, such as silhouettes and keypoints. These approaches guarantee a consistent 3D shape, however, the predefined shape covers only a limited number of animal categories, and the deformation space is constrained. On the other hand, model-free approaches, including [29, 30, 66, 9, 61, 60, 69, 24, 33, 2, 16, 65], learn a category-specific canonical shape from large-scale image datasets containing different instances of the same category. General-domain 4D reconstruction methods [16, 65] can also be applied to animals, but their reconstructed results lack part- or joint-level information, making them less flexible than animal-specific reconstruction approaches. At test time, they predict instance-specific pose and deformation parameters in a feed-forward manner. Additionally, 3D-Fauna [35] learns a generalizable prior shape bank from pan-category image data, aiming to predict category-agnostic prior shapes at test time. Model-free methods generally accommodate a more diverse range of shapes, however, their feed-forward nature at test time limits the accuracy of shape and pose reconstruction. In this work, we propose a new baseline method that combines the advantages of model-based and model-free approaches by directly optimizing per-frame parameters of a pretrained model-free model at test time, incorporating additional geometric and temporal loss terms on video data.

2.2 Web Data Collection

As machine learning models continue to scale rapidly, the demand for larger-scale datasets has become increasingly critical for effective training. The most effective approach to data collection is leveraging the vast amount of information available on the web, processing it into structured datasets tailored for specific tasks. The training of state-of-the-art language models [3, 22, 52] often relies on large-scale text datasets scraped from the web, such as Common Crawl. Large-scale image datasets sourced from the web [50, 17] have also served as foundational resources for modern computer vision research. In the domain of video, many datasets obtain video data from online video-sharing platforms such as YouTube, Flickr, and Tumblr. Datasets such as ActivityNet [20], Kinetics [25], and YouTube-8M [1] utilize online videos as sources for classification tasks. Other datasets, such as HD-VG-130M [57], HD-VILA-100M [64], TGIF [34], MiraData [23], HowTo100M [39], WebVid-2M [5], collect text-video paired data from online sources for tasks including video captioning, retrieval, and generation. For more specialized tasks, however, specific approaches or processing pipelines are required to process and filter video data, often incorporating human annotations. Instructional datasets such as COIN [53] and IKEA Video Manuals [37] require human annotators to use annotation tools to create labels for the data. VoxConverse [15] and VGG-Sound [14] propose carefully designed automatic pipelines for audio-visual data annotation, only requiring minimal human effort for verification. Similarly, for the specific task of 4D animal reconstruction, we aim to develop a scalable automated pipeline for data preparation and processing, eliminating the need for human annotation while minimizing human effort for verification.

2.3 Animal Datasets

Many vision datasets focus specifically on animals, primarily designed for the task of animal pose estimation, where models are expected to predict the spatial configuration of animals given an image or other modality data. Some datasets focus on specific animal categories such as dogs, birds, and monkeys [18, 27, 56, 70]. Others encompass a diverse range of animal species but are limited to images without video data [72, 11, 41, 62]. There are some video-based animal datasets, such as BADJA [8] and APT-36K [68], EgoPet [6]. However, they suffer from two key limitations. First, they remain small in scale—the largest among them, APT-36K, contains only 2.4k videos, each with 15 frames. Second, these datasets consist of unprocessed in-the-wild videos, where typical frames may include multiple overlapping animals, lack center-cropping, and omit essential data such as masks. As a result, these datasets are not fully prepared for the task of 4D animal reconstruction, making them unsuitable for direct use by 4D animal reconstruction methods. To develop a scalable solution that produces ready-to-use data for animal reconstruction, we leverage large-scale online video data and design an automatic pipeline to collect and process structured datasets ready for 4D animal reconstruction task.

3 Data Collection

We propose a multi-stage data engine that can automatically collect and process data for 4D animal reconstruction task. The process follows a pipeline that searches for video candidates, applies tracking algorithms for object-centric video crops, filters out unwanted tracks, and leverages off-the-shelf pretrained vision models to extract all necessary image features for animal reconstruction. At the core of our data engine lies a database that stores metadata of intermediate results collected or processed at different stages, enabling parallel execution of multiple processes running same or different stages. An overview of our data engine is shown in Figure 2

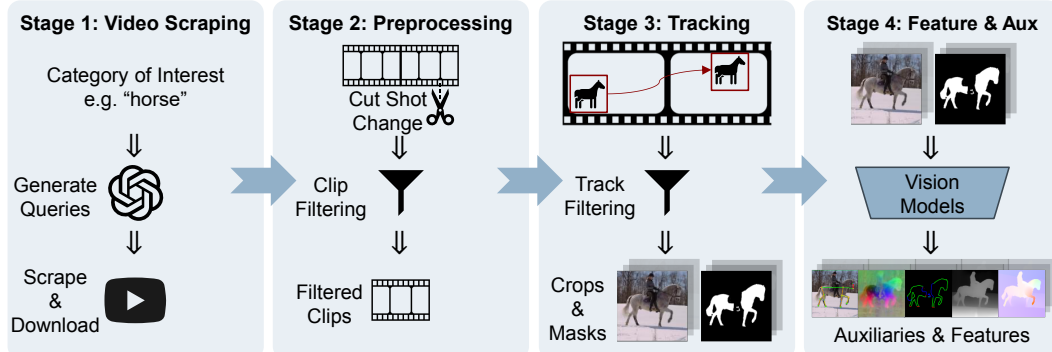


Figure 2: Overview of our proposed data pipeline. Data is automatically scraped from YouTube in stage 1, and then preprocessed into clips in stage 2. Stage 3 detects and tracks the instances, and the final stage extracts additional image features for 4D animal reconstruction.

3.1 Raw Video Collection

In this stage, we scrape and download raw videos from YouTube. We start with an arbitrary animal category or family, for example, horse, and leverage GPT to generate text search queries. To make search queries as diverse as possible, we first ask GPT to generate a set of more specific sub-category breeds, for example, *Clydesdale* and *Mustang*. Separately, GPT is asked to generate a set of context phrases that are related to the category of interests, for instance, *racing competition* and *in a farm* for horse. Finally, we randomly combine two sets to form a list of diverse search texts to query YouTube for raw videos. Our downloading pipeline is implemented based on *Selenium Webdriver* [51] for querying and retrieving video ID results and *pytube* [10] for downloading the videos.

3.2 Video Preprocessing

This stage aims to preprocess and prefilter the downloaded raw videos so that they are prepared for object tracking in the next stage. The final data we want should be object-centric crops of animals, but raw videos are typically noisy with many frames that do not have any animal of interest presented in the frame. We therefore split the video into video clips based on shot changes using PySceneDetect [13], which detects large values of weighted average pixel change across frames. Splitting videos by shot change also helps tracking as we observe that tracking algorithms may falsely associate objects in different shots. Next, we apply CLIP [45] and compute an average CLIPScore [21] between a randomly sampled batch of frames from the video clip and a text caption, for example, *a photo of a horse*, and discard video clips with low CLIPScore. This step filters out video clips that do not clearly depict the target animals, thereby eliminating the need for further tracking. All video clips are downsampled to 10 frames per second to enhance processing efficiency in later stages.

3.3 Animal Tracking

To obtain object-centric video cropping of an animal across frames, it is essential to track the same instance consistently over multiple frames. We employ Grounded-SAM-2 [47], which utilizes GroundingDINO [36] to detect object bounding boxes in each frame, serving as prompt inputs for SAM-2 [46] tracking. An iterative grounding-tracking process is applied to enable long-term tracking while also allowing the detection and tracking of newly appearing objects. After tracking, we obtain a set of object track proposals represented by their corresponding mask silhouettes from a video clip. We filter out any tracks that are potentially unsuitable for animal reconstruction task by applying the following filters and postprocessings.

Overlapping Instances. When multiple animals are present in a frame, off-the-shelf keypoint estimators may become confused and incorrectly assign keypoints to different instances, especially when significant overlap occurs. To mitigate this, we remove frames from tracks where two or more animals overlap substantially. We achieve this by thresholding the Intersection over Union (IoU) between each pair of animals in the same frame and removing both mask silhouettes from the tracks if their IoU exceeds the threshold.

Low Resolution Instances. If the animal is too small in the frame, subsequent operations such as keypoints and feature extraction may have degraded performance due to low resolution after resizing. Therefore we discard any frames from the track where the bounding box area of the animal is less than 1/4 of the final crop size, *e.g.* 256×256 if the final crop size is 512×512 .

Truncated Instances. In many cases, an animal’s full body is not visible within the video frame. Since animal reconstruction methods rely on mask silhouettes as shape supervision, truncated silhouettes can lead to inaccurate reconstructions with unnatural poses and shapes. We remove frames from the tracks if the bounding box is too close to the frame border, as these typically indicate a truncated animal.

Inconsistent Tracks. Tracking algorithms may fail when videos contain ambiguous cases or unnatural artifacts. A common failure occurs when multiple animals with similar appearances are present, causing the algorithm to switch identities and track different animals inconsistently. Another failure case arises from video fading effects, which are difficult to detect using shot detection algorithms in earlier stages. In some instances, the tracking algorithm may fail to stop even after a shot change or fade-out, continuing to track a different object or background in the new shot. To mitigate these issues, we apply a threshold on the bounding box IoU between adjacent frames of the same track and remove all frames following a detected low IoU.

Temporal Postprocessing. At this stage, some unqualified frames have been filtered from the tracking results, creating discontinuities. To address this, we apply a post-processing step based on predefined parameters for minimal track length, maximal track length, and the allowed gap within a track. By iterating through all frames in a track, we identify gaps exceeding the allowed threshold or instances where the track reaches the maximal length; in such cases, the subsequent frames are split into a new track. If a gap falls within the allowed threshold, we resegment missing mask silhouette

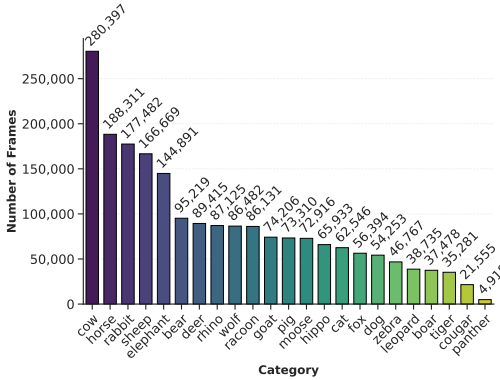


Figure 3: A detailed breakdown of the number of frames collected for each animal category in full dataset.

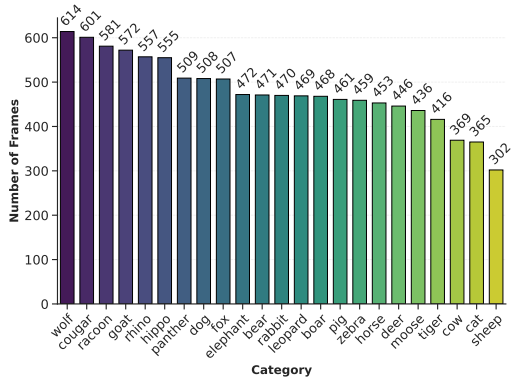


Figure 4: A detailed breakdown of the number of frames collected in benchmark data for each animal category.

using SAM-2, interpolating bounding boxes from both sides as input prompts. Any tracks shorter than the minimal track length are discarded.

Object-centric Cropping. To obtain the final object-centric video crops for animal reconstruction, we generate square crop boxes centered on the bounding box of the animal in each frame. The size of each crop box is determined by a predefined ratio relative to the mask area. We further apply moving average smoothing to the crop boxes before cropping and resizing all frames to a standardized size. As a final filtering step, we randomly select a cropped RGB image for each track and input it into GPT to identify and remove instances of false detection or heavily occluded animals.

3.4 Feature Extraction

Animal reconstruction methods typically rely on additional preprocessed features beyond RGB images to guide optimization. Most model-based approaches optimize shape and pose parameters to fit animal silhouettes and keypoints. Some methods [28] may also use optical flow as additional guidance. Model-free methods further incorporate precomputed image features such as DINO features [69, 61, 35]. While animal silhouettes are already obtained in a previous stage, our data pipeline modularly integrates off-the-shelf vision models to automatically infer animal keypoints, PCA DINO features, optical flow, and depth. Specifically, we integrate ViTPose++ [63] for animal keypoints estimation, DINOv2 [43] for image feature, SEA-RAFT [59] for optical flow estimation, and Depth Anything V2 [67] for depth estimation. Additionally, we compute occlusion boundaries for each animal crop based on the estimated depth and mask silhouette. Specifically, we extract depth values at the dilated and eroded mask boundaries, respectively. For each pixel on the original mask boundary, we calculate the depth difference between the nearest pixel on the dilated boundary and the nearest pixel on the eroded boundary. This depth difference helps determine whether the pixels outside the animal silhouette belong to the foreground, indicating occlusion, or the background, indicating no occlusion at that region. Using the estimated optical flow and occlusion boundaries, we can optionally further filter the processed data to retain instances with greater motion and minimal occlusion.

3.5 Dataset Statistics

Using the proposed automated data pipeline, we can efficiently collect a large volume of structured video data suitable for 4D animal reconstruction. We have successfully collected and processed 29,979 animal video data, totaling 2,046,414 frames. Specifically, we begin with 23 common animal categories as input to our data engine, and we present category statistics in Figure 9. A typical data sample collected is shown in Figure 5.

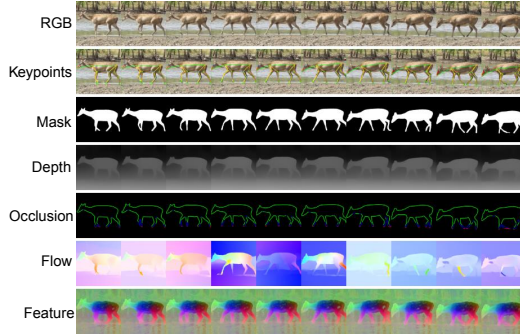


Figure 5: Visualization of a collected data sample. Each video is annotated per frame with keypoints, mask silhouettes, depth maps, occlusion boundaries, optical flow, and DINO features.

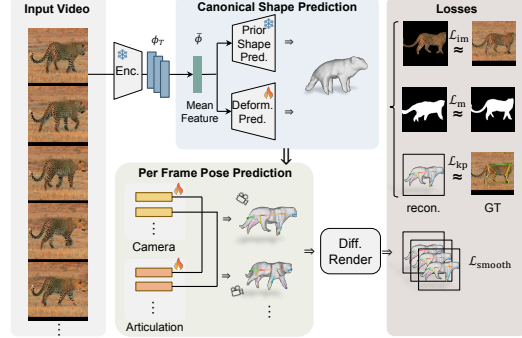


Figure 6: Overview of 4D-Fauna. We adapt 3D-Fauna [35] to enhance its capability for direct sequence optimization.

4 4D Animal Reconstruction

Using our proposed data engine, we can generate large-scale datasets for 4D animal reconstruction. To demonstrate its effectiveness, we establish a benchmark dataset, Animal-in-Motion, for evaluating 4D animal reconstruction methods. In this section, we detail the task of 4D animal reconstruction, the construction process of the benchmark dataset, and the evaluation metrics. Additionally, we propose a novel baseline method, 4D-Fauna, that adapts 3D-Fauna [35] with additional loss terms, enhancing its suitability for direct sequence optimization while combining the strengths of both traditional model-based and model-free approaches. Finally, we present benchmarking results comparing a typical model-based method, a model-free method, and our proposed baseline method.

4.1 Task Formulation

Similar to the 3D animal reconstruction task, which aims to estimate an animal’s 3D pose and shape from a single image, the 4D animal reconstruction task seeks to estimate a sequence of 3D poses and shapes from a sequence of frames of the same animal. Beside RGB image input, typical methods also require other 2D auxiliary data as guidance, such as mask silhouettes and 2D keypoints, obtained either from manual labeling or from pretrained vision models. Formally, given an RGB video input $\mathcal{V}_T = \{v_t\}_{t=1}^T \in \mathbb{R}^{T \times 3 \times H \times W}$ of an animal, along with any required auxiliary input $\mathcal{A}_T = \{a_t\}_{t=1}^T$, in $\{0, 1\}^{T \times H \times W}$ in the case of 2D mask or in $\mathbb{R}^{T \times K \times 2}$ in the case of 2D keypoints for instance, a function $f_\theta : \{\mathcal{V}, \mathcal{A}\} \mapsto \mathcal{S}$ is expected to output a sequence of posed 3D shapes $\mathcal{S}_T = \{s_t\}_{t=1}^T$ that naturally resembles the shape and pose sequence shown in the input video \mathcal{V}_T , where T is number of frames in sequence, H and W are spatial dimensions of the frames, K is number of defined keypoints. Function f_θ can operate either as a feed-forward model using pretrained parameter θ , or by optimizing θ at test time. Since different methods operate differently—some requiring large-scale training data [35] while others only perform test-time optimization [74, 7]—our benchmark dataset is designed for evaluation only to ensure fair comparisons.

4.2 Benchmark Dataset

Using the data pipeline proposed in Section 3, we can effortlessly collect large-scale data for the 4D animal reconstruction task from scratch. However, to establish a benchmark, it is crucial to ensure the accuracy of all annotations. This is achieved through human validation, requiring minimal effort from annotators, who simply accept or reject a data sample by reviewing three auxiliary visualizations generated by the data pipeline: the RGB video, RGB video applied with per frame mask silhouette, and RGB video overlayed with per frame keypoints visualization. The criteria for accepting a data sample are as follows:

- The RGB video does not exhibit heavy occlusion of the animal by other objects, particularly on the legs, though self-occlusion is allowed.

- The RGB video displays recognizable and smooth motion in animal body parts.
- The RGB video displays smooth camera movement.
- The RGB video applied with per frame mask silhouettes correctly segments the animal without significant missing body parts.
- The RGB video overlayed with per frame keypoints accurately and smoothly approximates the animal’s joint positions across frames.

As a result, we curate 10 videos per category, yielding a total of 230 videos comprising 11,061 frames. A detailed breakdown of the frame statistics is presented in Figure 4.

4.3 Metrics

It is non-trivial to evaluate a 2D-to-3D lifting task since there is no 3D ground truth data. However, literatures have used different proxies to evaluate.

Silhouette Intersection-over-union (IoU). We follow previous works [9, 76, 4, 53, 49, 69] to employ silhouette intersection-over-union (IoU). Silhouette IoU measure the IoU between the ground truth silhouette mask and the silhouette mask rendered by the reconstructed 3D shape. Although a high 2D IoU does not necessarily correspond to a natural 3D shape due to potential ambiguities, a low IoU reliably indicates that the reconstruction is underperforming.

Percentage of Correct Keypoint (PCK). Following previous works [24, 33, 30, 60, 61, 35], we use the Percentage of Correct Keypoints (PCK) metric, which measures the percentage of projected keypoints that fall within a fixed multiple of a normalizing distance threshold. Studies have defined different distance thresholds. Following [9, 31, 8], we use the square root of the ground-truth mask silhouette area as the normalizing distance threshold.

Keypoint Transfer (KT). Since no ground-truth 3D keypoint or shape annotations exist, previous works [61, 35, 29, 30, 69, 33, 8, 28] use Keypoint Transfer (KT) as a proxy for evaluating reconstructed 3D shapes. Specifically, a set of ground-truth 2D keypoints from a source image is projected onto the reconstructed 3D shape surface to establish a mapping with surface vertices. The corresponding vertices are then reprojected from the 3D shape onto a target image with novel view and pose. PCK is computed using the reprojected keypoints and the ground-truth keypoints in the target image. A well-reconstructed 3D shape should exhibit consistency, producing low errors after undergoing this 2D-to-3D-to-2D mapping.

Mean Per-Joint Velocity Error (MPJVE). As our work is the first to specifically focus on the task of 4D animal reconstruction, there are no established metrics for evaluating reconstructed motion in the temporal dimension. Following related works in human motion estimation [44, 54, 73], we adopt Mean Per-Joint Velocity Error (MPJVE) to quantify the discrepancy in joint velocity within the projected, normalized pixel space. Specifically, for each joint across two consecutive frames, we compute the magnitude of the vector difference between the ground-truth velocity and the predicted velocity. The final MPJVE is obtained by averaging the error over all joints and all frames.

4.4 4D-Fauna

We propose 4D-Fauna, a new baseline for 4D animal reconstruction, which adapts 3D-Fauna [35], a model-free reconstruction approach designed for pan-category quadruped 3D reconstruction. Figure 6 gives an overview of our method.

Preliminary. 3D-Fauna builds upon MagicPony [61], which learns a prior shape for a specific animal category from diverse images of that category by leveraging self-supervised DINO-ViT [12] features. It then applies instance-specific predicted parameters, such as deformation and articulation, for inverse rendering supervision. Building on this, 3D-Fauna introduces a learnable prior shape bank, which functions as a dictionary of features capable of dynamically combining basis shapes during training and inference to generate diverse instance-specific prior 3D shapes. As a result, 3D-Fauna removes the constraint of training and inference on a single category, enabling it to learn a rich prior shape bank from pan-category images and produce diverse prior shapes at inference time.

Method	IoU \uparrow	PCK@0.1 \uparrow	PCK@0.05 \uparrow	KT-PCK@0.1 \uparrow	KT-PCK@0.05 \uparrow	MPJVE \downarrow
SMALify [7]	0.867	0.954	0.787	0.623	0.372	0.023
AniMer [38]	0.677	0.537	0.199	0.566	0.256	0.038
3D-Fauna [35]	0.670	0.470	0.177	0.329	0.130	0.058
4D-Fauna	0.814	0.664	0.317	0.418	0.193	0.044

Table 1: Benchmark results comparison of different 4D animal reconstruction methods. blue represents model-based approach and red indicates model-free approach.

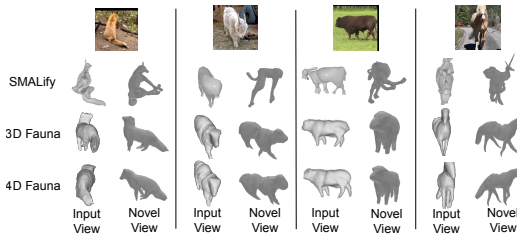


Figure 7: Comparison of 3D reconstruction results highlighting failure cases of SMALify.

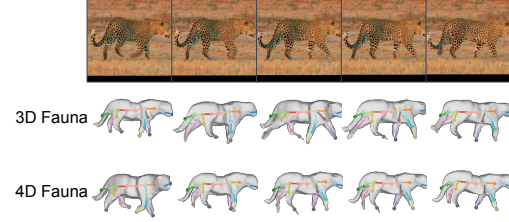


Figure 8: Comparison of 4D reconstruction results highlighting failure cases of 3D-Fauna.

Sequence Optimization. 3D-Fauna operates in a feed-forward manner, differing from traditional model-based approaches that iteratively optimize a predefined shape to fit a single image through inverse rendering. Consequently, it may yield suboptimal shape and pose fitting compared to model-based methods that overfit to the 2D supervision. To address this, we leverage the pretrained 3D-Fauna and perform per-sequence optimization for 4D reconstruction. However, directly optimizing on a sequence presents several challenges as follows.

Pose Ambiguity. Since 3D-Fauna relies solely on 2D mask supervision for the entire projected silhouette without any part-level constraints, the reconstructed results often fail to accurately preserve the correct leg ordering in the image. This error becomes more pronounced in video reconstruction, leading to unnatural gait cycles where the legs fail to switch properly when the animal is walking or running, particularly in side-view perspectives. To address this issue, we explicitly incorporate 2D keypoint annotations as part-level supervision during sequence optimization, similar to how keypoint reprojection loss is utilized in model-based approaches.

Temporal Smoothness. We apply temporal smoothness loss terms on both the camera pose and animal pose. Specifically, we regularize the magnitude of change in camera pose parameters and velocity of animal pose articulation.

Efficient Overfitting. 3D-Fauna uses neural network predictors to predict camera pose and articulation parameters from input image features. To efficiently overfit camera pose and articulation for the sequence, we directly optimize the camera pose and articulation parameters for each frame, taking the output from pretrained neural network predictors as initialization.

4.5 Results and Analysis

We show benchmark results of 4D-Fauna, 3D-Fauna [35], SMALify [7], which is a model-base reconstruction approach that implements [8] and [9], and AniMer [38], which is a model-base feedforward reconstruction method. The quantitative results are reported in Table 1.

As a model-based method, SMALify achieves the best results across all metrics. This is because model-based methods explicitly optimize pose and shape deformation to align with 2D ground truth, leading to superior performance on 2D metrics. However, this optimization process is not inherently 3D-aware—i.e., it does not learn general animal pose and shape representations from diverse data. As a result, when fitting to 2D supervision, the method often produces unnatural poses and shapes due to ambiguities in the depth dimension. Some failure cases of SMALify are illustrated in Figure 7.

The first column from the left illustrates an incorrect pose prediction. Since both the correct and incorrect poses can perfectly fit the 2D mask silhouette and keypoints, the model fails to differentiate between them in this case. The second column demonstrates that in the depth dimension, SMALify may arbitrarily elongate body parts, as such distortions are not apparent in the projected 2D shape. The third column presents a similar failure due to depth ambiguity, where the legs unnaturally bend sideways in 3D space to conform to the 2D supervision. The last column highlights how SMALify drastically deforms the shape into an unnatural configuration to perfectly fit a frontal-view image. In contrast, both 3D-Fauna and 4D-Fauna effectively infer plausible 3D shapes and natural poses. Moreover, 4D-Fauna generally achieves more accurate camera and animal pose fitting than 3D-Fauna, thanks to further sequence-level optimization.

From quantitative results and qualitative assessments shown in Figures 7 and 8, 4D-Fauna achieves better performance on all metrics than 3D-Fauna while maintaining plausible and natural 3D shape and pose. Specifically, further optimization using mask silhouette supervision contributes to a higher IoU, promoting improved per-frame pose estimation and more accurate shape deformation for individual instances. Although the joint definitions are not fully aligned, direct keypoint supervision on joints with overlapping definitions is sufficient to reconstruct a more accurate animal pose, leading to a higher PCK score. Furthermore, improved camera and animal pose estimation together enhance Keypoint Transfer accuracy in the 2D-to-3D-to-2D mapping process. Additionally, loss terms for motion smoothness help reduce jitter and sudden large movements, producing a more stable and realistic motion that closely resembles the ground truth. A comparison of 4D reconstruction result is shown in Figure 8. Comparing the two model-free approaches, 3D-Fauna exhibits sudden leg switching between frames 2 and 4 in Figure 8, whereas 4D-Fauna successfully resolves this issue, highlighting the necessity of further sequence optimization with keypoint supervision and smoothness loss terms.

5 Conclusion

We present a fully automated, scalable data pipeline for 4D quadruped animal reconstruction. We introduce Animal-in-Motion, the first benchmark for 4D animal shape and pose estimation, and establish a thorough evaluation framework for existing 3D reconstruction approaches. Additionally, we propose 4D-Fauna, a baseline that boosts model-free reconstruction accuracy. Our results show the pipeline’s ability to generate high-quality data, also highlighting the importance of 3D-aware evaluation and visualization on the animal reconstruction task, opening avenues for further advances in shape and motion understanding of animals.

Limitation. While our pipeline significantly reduces the human effort required for large-scale animal video collection and annotation, the automatically processed data is not perfectly clean and still requires manual validation for reliable benchmarking. Our benchmark dataset, though curated, relies on 2D projection-based metrics, which are limited by inherent view ambiguities and do not fully capture 3D reconstruction quality—highlighting the need for more robust, 3D-aware evaluation metrics. Finally, our baseline builds on an existing model-free method with temporal refinements, but it demonstrates only limited understanding of temporal coherence; future approaches may benefit from more expressive paradigms, such as autoregressive models, to better capture inter-frame dynamics.

Accessibility. The source code and instructions to download dataset are available on GitHub: <https://github.com/briannlongzhao/Animal-in-Motion>

Our dataset includes annotations derived from publicly available YouTube videos. We acknowledge that YouTube content is subject to copyright protection and governed by YouTube’s Terms of Service. To respect these terms and mitigate copyright and privacy concerns, we do not release the original RGB video frames. Instead, we publicly release only derived data, such as mask, depth, keypoints, *etc.*, which do not contain any raw video content. All derived data is non-identifiable and used solely for research purposes. We also provide scripts to re-derive necessary data and visualizations locally, ensuring reproducibility for research purpose.

Acknowledgments and Disclosure of Funding

This work is in part supported by ONR MURI N00014-22-1-2740, NSF RI #2211258, and #2338203.

References

- [1] Sami Abu-El-Haija, Nisarg Kothari, Joonseok Lee, Paul Natsev, George Toderici, Balakrishnan Varadarajan, and Sudheendra Vijayanarasimhan. Youtube-8m: A large-scale video classification benchmark. *arXiv preprint arXiv:1609.08675*, 2016.
- [2] Antonio Agudo. Safari from visual signals: Recovering volumetric 3d shapes. In *ICASSP 2022 - 2022 IEEE International Conference on Acoustics, Speech and Signal Processing (ICASSP)*, pages 2495–2499, 2022.
- [3] Anthropic. The claude 3 model family: Opus, sonnet, haiku, 2024. Accessed: March 1, 2025.
- [4] Marc Badger, Yufu Wang, Adarsh Modh, Ammon Perkes, Nikos Kolotouros, Bernd G Pfommer, Marc F Schmidt, and Kostas Daniilidis. 3d bird reconstruction: a dataset, model, and shape recovery from a single view. In *European conference on computer vision*, pages 1–17. Springer, 2020.
- [5] Max Bain, Arsha Nagrani, GüL Varol, and Andrew Zisserman. Frozen in time: A joint video and image encoder for end-to-end retrieval. In *Proceedings of the IEEE/CVF international conference on computer vision*, pages 1728–1738, 2021.
- [6] Amir Bar, Arya Bakhtiar, Danny Tran, Antonio Loquercio, Jathushan Rajasegaran, Yann LeCun, Amir Globerson, and Trevor Darrell. Egopet: Egomotion and interaction data from an animal’s perspective. In *European Conference on Computer Vision*, pages 377–394. Springer, 2024.
- [7] Benjiebob. Smalify: A method for 3d animal shape reconstruction. <https://github.com/benjiebob/SMALify>, 2025. Accessed: 2025-02-28.
- [8] Benjamin Biggs, Thomas Roddick, Andrew Fitzgibbon, and Roberto Cipolla. Creatures great and smal: Recovering the shape and motion of animals from video. In *Computer Vision–ACCV 2018: 14th Asian Conference on Computer Vision, Perth, Australia, December 2–6, 2018, Revised Selected Papers, Part V 14*, pages 3–19. Springer, 2019.
- [9] Benjamin Biggs, Oliver Boyne, James Charles, Andrew Fitzgibbon, and Roberto Cipolla. Who left the dogs out? 3d animal reconstruction with expectation maximization in the loop. In *Computer Vision–ECCV 2020: 16th European Conference, Glasgow, UK, August 23–28, 2020, Proceedings, Part XI 16*, pages 195–211. Springer, 2020.
- [10] Juan Bindez. pytubefix: Python3 library for downloading youtube videos, 2025. Version 8.12.2, accessed: 2025-03-01.
- [11] Jinkun Cao, Hongyang Tang, Hao-Shu Fang, Xiaoyong Shen, Cewu Lu, and Yu-Wing Tai. Cross-domain adaptation for animal pose estimation. In *Proceedings of the IEEE/CVF international conference on computer vision*, pages 9498–9507, 2019.
- [12] Mathilde Caron, Hugo Touvron, Ishan Misra, Hervé Jégou, Julien Mairal, Piotr Bojanowski, and Armand Joulin. Emerging properties in self-supervised vision transformers. In *Proceedings of the IEEE/CVF international conference on computer vision*, pages 9650–9660, 2021.
- [13] Brandon Castellano. Pyscenedetect: Video scene detection and analysis tool, 2024. Accessed: 2025-03-01.
- [14] Honglie Chen, Weidi Xie, Andrea Vedaldi, and Andrew Zisserman. Vggsound: A large-scale audio-visual dataset. In *ICASSP 2020-2020 IEEE International Conference on Acoustics, Speech and Signal Processing (ICASSP)*, pages 721–725. IEEE, 2020.
- [15] Joon Son Chung, Jaesung Huh, Arsha Nagrani, Triantafyllos Afouras, and Andrew Zisserman. Spot the conversation: speaker diarisation in the wild. *Interspeech*, 2020.
- [16] Sergio M de Paco and Antonio Agudo. 4dpv: 4d pet from videos by coarse-to-fine non-rigid radiance fields. In *Proceedings of the Asian Conference on Computer Vision*, pages 2596–2612, 2024.
- [17] Jia Deng, Wei Dong, Richard Socher, Li-Jia Li, Kai Li, and Li Fei-Fei. Imagenet: A large-scale hierarchical image database. In *2009 IEEE Conference on Computer Vision and Pattern Recognition*, pages 248–255, 2009.
- [18] Nisarg Desai, Praneet Bala, Rebecca Richardson, Jessica Raper, Jan Zimmermann, and Benjamin Hayden. Openapepose, a database of annotated ape photographs for pose estimation. *Elife*, 12:RP86873, 2023.
- [19] Semih Günel, Helge Rhodin, Daniel Morales, João Compagnolo, Pavan Ramdy, and Pascal Fua. Deepfly3d, a deep learning-based approach for 3d limb and appendage tracking in tethered, adult drosophila. In *eLife*, 2019.

[20] Fabian Caba Heilbron, Victor Escorcia, Bernard Ghanem, and Juan Carlos Niebles. Activitynet: A large-scale video benchmark for human activity understanding. In *2015 IEEE Conference on Computer Vision and Pattern Recognition (CVPR)*, pages 961–970, 2015.

[21] Jack Hessel, Ari Holtzman, Maxwell Forbes, Ronan Le Bras, and Yejin Choi. Clipscore: A reference-free evaluation metric for image captioning. *arXiv preprint arXiv:2104.08718*, 2021.

[22] Aaron Hurst, Adam Lerer, Adam P Goucher, Adam Perelman, Aditya Ramesh, Aidan Clark, AJ Ostrow, Akila Welihinda, Alan Hayes, Alec Radford, et al. Gpt-4o system card. *arXiv preprint arXiv:2410.21276*, 2024.

[23] Xuan Ju, Yiming Gao, Zhaoyang Zhang, Ziyang Yuan, Xintao Wang, Ailing Zeng, Yu Xiong, Qiang Xu, and Ying Shan. Miradata: A large-scale video dataset with long durations and structured captions. *Advances in Neural Information Processing Systems*, 37:48955–48970, 2025.

[24] Angjoo Kanazawa, Shubham Tulsiani, Alexei A Efros, and Jitendra Malik. Learning category-specific mesh reconstruction from image collections. In *Proceedings of the European conference on computer vision (ECCV)*, pages 371–386, 2018.

[25] Will Kay, Joao Carreira, Karen Simonyan, Brian Zhang, Chloe Hillier, Sudheendra Vijayanarasimhan, Fabio Viola, Tim Green, Trevor Back, Paul Natsev, et al. The kinetics human action video dataset. *arXiv preprint arXiv:1705.06950*, 2017.

[26] Sinead Kearney, Wenbin Li, Martin Parsons, Kwang In Kim, and Darren Cosker. Rgbd-dog: Predicting canine pose from rgbd sensors. In *Proceedings of the IEEE/CVF conference on computer vision and pattern recognition*, pages 8336–8345, 2020.

[27] Aditya Khosla, Nityananda Jayadevaprakash, Bangpeng Yao, and Li Fei-Fei. Novel dataset for fine-grained image categorization. In *First Workshop on Fine-Grained Visual Categorization, IEEE Conference on Computer Vision and Pattern Recognition*, Colorado Springs, CO, 2011.

[28] Filippos Kokkinos and Iasonas Kokkinos. Learning monocular 3d reconstruction of articulated categories from motion. In *Proceedings of the IEEE/CVF Conference on Computer Vision and Pattern Recognition*, pages 1737–1746, 2021.

[29] Nilesh Kulkarni, Abhinav Gupta, and Shubham Tulsiani. Canonical surface mapping via geometric cycle consistency. In *Proceedings of the IEEE/CVF International Conference on Computer Vision*, pages 2202–2211, 2019.

[30] Nilesh Kulkarni, Abhinav Gupta, David F Fouhey, and Shubham Tulsiani. Articulation-aware canonical surface mapping. In *Proceedings of the IEEE/CVF Conference on Computer Vision and Pattern Recognition*, pages 452–461, 2020.

[31] Chen Li and Gim Hee Lee. Coarse-to-fine animal pose and shape estimation. *Advances in Neural Information Processing Systems*, 34:11757–11768, 2021.

[32] Ci Li, Ylva Mellbin, Johanna Krogager, Senya Polikovsky, Martin Holmberg, Nima Ghorbani, Michael J Black, Hedvig Kjellström, Silvia Zuffi, and Elin Hernlund. The poses for equine research dataset (pferd). *Scientific Data*, 11(1):497, 2024.

[33] Xueting Li, Sifei Liu, Kihwan Kim, Shalini De Mello, Varun Jampani, Ming-Hsuan Yang, and Jan Kautz. Self-supervised single-view 3d reconstruction via semantic consistency. In *ECCV*, 2020.

[34] Yuncheng Li, Yale Song, Liangliang Cao, Joel Tetreault, Larry Goldberg, Alejandro Jaimes, and Jiebo Luo. Tgif: A new dataset and benchmark on animated gif description. In *Proceedings of the IEEE Conference on Computer Vision and Pattern Recognition*, pages 4641–4650, 2016.

[35] Zizhang Li, Dor Litvak, Ruining Li, Yunzhi Zhang, Tomas Jakab, Christian Rupprecht, Shangzhe Wu, Andrea Vedaldi, and Jiajun Wu. Learning the 3d fauna of the web. In *Proceedings of the IEEE/CVF Conference on Computer Vision and Pattern Recognition (CVPR)*, pages 9752–9762, 2024.

[36] Shilong Liu, Zhaoyang Zeng, Tianhe Ren, Feng Li, Hao Zhang, Jie Yang, Chunyuan Li, Jianwei Yang, Hang Su, Jun Zhu, et al. Grounding dino: Marrying dino with grounded pre-training for open-set object detection. *arXiv preprint arXiv:2303.05499*, 2023.

[37] Yunong Liu, Cristobal Eyzaguirre, Manling Li, Shubh Khanna, Juan Carlos Niebles, Vineeth Ravi, Saumitra Mishra, Weiyu Liu, and Jiajun Wu. IKEA manuals at work: 4d grounding of assembly instructions on internet videos. In *The Thirty-eighth Conference on Neural Information Processing Systems Datasets and Benchmarks Track*, 2024.

[38] Jin Lyu, Tianyi Zhu, Yi Gu, Li Lin, Pujin Cheng, Yebin Liu, Xiaoying Tang, and Liang An. Animer: Animal pose and shape estimation using family aware transformer. In *Proceedings of the Computer Vision and Pattern Recognition Conference*, pages 17486–17496, 2025.

[39] Antoine Miech, Dimitri Zhukov, Jean-Baptiste Alayrac, Makarand Tapaswi, Ivan Laptev, and Josef Sivic. Howto100m: Learning a text-video embedding by watching hundred million narrated video clips. In *Proceedings of the IEEE/CVF international conference on computer vision*, pages 2630–2640, 2019.

[40] Hemal Naik, Alex Hoi Hang Chan, Junran Yang, Mathilde Delacoux, Iain D Couzin, Fumihiro Kano, and Máté Nagy. 3d-pop-an automated annotation approach to facilitate markerless 2d-3d tracking of freely moving birds with marker-based motion capture. In *Proceedings of the IEEE/CVF conference on computer vision and pattern recognition*, pages 21274–21284, 2023.

[41] Xun Long Ng, Kian Eng Ong, Qichen Zheng, Yun Ni, Si Yong Yeo, and Jun Liu. Animal kingdom: A large and diverse dataset for animal behavior understanding. In *Proceedings of the IEEE/CVF Conference on Computer Vision and Pattern Recognition (CVPR)*, pages 19023–19034, 2022.

[42] Tomasz Niewiadomski, Anastasios Yiannakidis, Hanz Cuevas-Velasquez, Soubhik Sanyal, Michael J Black, Silvia Zuffi, and Peter Kulits. Generative zoo. *arXiv preprint arXiv:2412.08101*, 2024.

[43] Maxime Oquab, Timothée Darcet, Theo Moutakanni, Huy V. Vo, Marc Szafraniec, Vasil Khalidov, Pierre Fernandez, Daniel Haziza, Francisco Massa, Alaaeldin El-Nouby, Russell Howes, Po-Yao Huang, Hu Xu, Vasu Sharma, Shang-Wen Li, Wojciech Galuba, Mike Rabbat, Mido Assran, Nicolas Ballas, Gabriel Synnaeve, Ishan Misra, Herve Jegou, Julien Mairal, Patrick Labatut, Armand Joulin, and Piotr Bojanowski. Dinov2: Learning robust visual features without supervision, 2023.

[44] Dario Pavllo, Christoph Feichtenhofer, David Grangier, and Michael Auli. 3d human pose estimation in video with temporal convolutions and semi-supervised training. In *Proceedings of the IEEE/CVF conference on computer vision and pattern recognition*, pages 7753–7762, 2019.

[45] Alec Radford, Jong Wook Kim, Chris Hallacy, Aditya Ramesh, Gabriel Goh, Sandhini Agarwal, Girish Sastry, Amanda Askell, Pamela Mishkin, Jack Clark, et al. Learning transferable visual models from natural language supervision. In *International conference on machine learning*, pages 8748–8763. PMLR, 2021.

[46] Nikhila Ravi, Valentin Gabeur, Yuan-Ting Hu, Ronghang Hu, Chaitanya Ryali, Tengyu Ma, Haitham Khedr, Roman Rädle, Chloe Rolland, Laura Gustafson, Eric Mintun, Junting Pan, Kalyan Vasudev Alwala, Nicolas Carion, Chao-Yuan Wu, Ross Girshick, Piotr Dollár, and Christoph Feichtenhofer. Sam 2: Segment anything in images and videos. *arXiv preprint arXiv:2408.00714*, 2024.

[47] Tianhe Ren, Shilong Liu, Ailing Zeng, Jing Lin, Kunchang Li, He Cao, Jiayu Chen, Xinyu Huang, Yukang Chen, Feng Yan, Zhaoyang Zeng, Hao Zhang, Feng Li, Jie Yang, Hongyang Li, Qing Jiang, and Lei Zhang. Grounded sam: Assembling open-world models for diverse visual tasks, 2024.

[48] Nadine Rueegg, Silvia Zuffi, Konrad Schindler, and Michael J Black. Barc: Learning to regress 3d dog shape from images by exploiting breed information. In *Proceedings of the IEEE/CVF Conference on Computer Vision and Pattern Recognition*, pages 3876–3884, 2022.

[49] Nadine Rueegg, Shashank Tripathi, Konrad Schindler, Michael J. Black, and Silvia Zuffi. Bite: Beyond priors for improved three-d dog pose estimation. In *2023 IEEE/CVF Conference on Computer Vision and Pattern Recognition (CVPR)*, pages 8867–8876, 2023.

[50] Christoph Schuhmann, Romain Beaumont, Richard Vencu, Cade Gordon, Ross Wightman, Mehdi Cherti, Theo Coombes, Aarush Katta, Clayton Mullis, Mitchell Wortsman, et al. Laion-5b: An open large-scale dataset for training next generation image-text models. *Advances in neural information processing systems*, 35:25278–25294, 2022.

[51] SeleniumHQ. Selenium webdriver, 2025. Accessed: 2025-03-01.

[52] Zhihong Shao, Peiyi Wang, Qihao Zhu, Runxin Xu, Junxiao Song, Xiao Bi, Haowei Zhang, Mingchuan Zhang, YK Li, Y Wu, et al. Deepseekmath: Pushing the limits of mathematical reasoning in open language models. *arXiv preprint arXiv:2402.03300*, 2024.

[53] Yansong Tang, Dajun Ding, Yongming Rao, Yu Zheng, Danyang Zhang, Lili Zhao, Jiwen Lu, and Jie Zhou. Coin: A large-scale dataset for comprehensive instructional video analysis. In *Proceedings of the IEEE/CVF Conference on Computer Vision and Pattern Recognition*, pages 1207–1216, 2019.

[54] Mansour Tchenegnon, Sylvie Gibet, and Thibaut Le Naour. A new spatio-temporal loss function for 3d motion reconstruction and extended temporal metrics for motion evaluation. *arXiv preprint arXiv:2210.08562*, 2022.

[55] Gemini Team, Rohan Anil, Sebastian Borgeaud, Jean-Baptiste Alayrac, Jiahui Yu, Radu Soricu, Johan Schalkwyk, Andrew M Dai, Anja Hauth, Katie Millican, et al. Gemini: a family of highly capable multimodal models. *arXiv preprint arXiv:2312.11805*, 2023.

[56] C. Wah, S. Branson, P. Welinder, P. Perona, and S. Belongie. Caltech-ucsd birds-200-2011. Technical Report CNS-TR-2011-001, California Institute of Technology, 2011.

[57] Wenjing Wang, Huan Yang, Zixi Tuo, Huiguo He, Junchen Zhu, Jianlong Fu, and Jiaying Liu. Swap attention in spatiotemporal diffusions for text-to-video generation. *International Journal of Computer Vision*, pages 1–19, 2025.

[58] Yufu Wang, Nikos Kolotouros, Kostas Daniilidis, and Marc Badger. Birds of a feather: Capturing avian shape models from images. In *Proceedings of the IEEE/CVF Conference on Computer Vision and Pattern Recognition*, pages 14739–14749, 2021.

[59] Yihan Wang, Lahav Lipson, and Jia Deng. Sea-raft: Simple, efficient, accurate raft for optical flow. In *European Conference on Computer Vision*, pages 36–54. Springer, 2024.

[60] Shangzhe Wu, Tomas Jakab, Christian Rupprecht, and Andrea Vedaldi. Dove: Learning deformable 3d objects by watching videos. *International Journal of Computer Vision*, 131(10):2623–2634, 2023.

[61] Shangzhe Wu, Ruining Li, Tomas Jakab, Christian Rupprecht, and Andrea Vedaldi. MagicPony: Learning articulated 3d animals in the wild. In *CVPR*, 2023.

[62] Jiacong Xu, Yi Zhang, Jiawei Peng, Wufei Ma, Artur Jesslen, Pengliang Ji, Qixin Hu, Jiehua Zhang, Qihao Liu, Jiahao Wang, et al. Animal3d: A comprehensive dataset of 3d animal pose and shape. *arXiv preprint arXiv:2308.11737*, 2023.

[63] Yufei Xu, Jing Zhang, Qiming Zhang, and Dacheng Tao. Vitpose++: Vision transformer for generic body pose estimation. *IEEE Transactions on Pattern Analysis and Machine Intelligence*, 46(2):1212–1230, 2023.

[64] Hongwei Xue, Tiankai Hang, Yanhong Zeng, Yuchong Sun, Bei Liu, Huan Yang, Jianlong Fu, and Baining Guo. Advancing high-resolution video-language representation with large-scale video transcriptions. In *Proceedings of the IEEE/CVF Conference on Computer Vision and Pattern Recognition*, pages 5036–5045, 2022.

[65] Gengshan Yang, Deqing Sun, Varun Jampani, Daniel Vlasic, Forrester Cole, Ce Liu, and Deva Ramanan. Viser: Video-specific surface embeddings for articulated 3d shape reconstruction. In *NeurIPS*, 2021.

[66] Gengshan Yang, Minh Vo, Natalia Neverova, Deva Ramanan, Andrea Vedaldi, and Hanbyul Joo. Banmo: Building animatable 3d neural models from many casual videos. In *Proceedings of the IEEE/CVF Conference on Computer Vision and Pattern Recognition*, pages 2863–2873, 2022.

[67] Lihe Yang, Bingyi Kang, Zilong Huang, Zhen Zhao, Xiaogang Xu, Jiashi Feng, and Hengshuang Zhao. Depth anything v2. *Advances in Neural Information Processing Systems*, 37:21875–21911, 2025.

[68] Yuxiang Yang, Junjie Yang, Yufei Xu, Jing Zhang, Long Lan, and Dacheng Tao. Apt-36k: A large-scale benchmark for animal pose estimation and tracking. *Advances in Neural Information Processing Systems*, 35:17301–17313, 2022.

[69] Chun-Han Yao, Wei-Chih Hung, Yuanzhen Li, Michael Rubinstein, Ming-Hsuan Yang, and Varun Jampani. Lassie: Learning articulated shape from sparse image ensemble via 3d part discovery. In *NeurIPS*, 2022.

[70] Yuan Yao, Praneet Bala, Abhiraj Mohan, Eliza Bliss-Moreau, Kristine Coleman, Sienna M. Freeman, Christopher J. Machado, Jessica Raper, Jan Zimmermann, Benjamin Y. Hayden, and Hyun Soo Park. Openmonkeychallenge: Dataset and benchmark challenges for pose estimation of non-human primates. *Int. J. Comput. Vision*, 131(1):243–258, 2022.

[71] Tarik Yigit, Feng Han, Ellen Rankins, Jingang Yi, Kenneth H. McKeever, and Karyn Malinowski. Wearable inertial sensor-based limb lameness detection and pose estimation for horses. *IEEE Transactions on Automation Science and Engineering*, 19(3):1365–1379, 2022.

[72] Hang Yu, Yufei Xu, Jing Zhang, Wei Zhao, Ziyu Guan, and Dacheng Tao. Ap-10k: A benchmark for animal pose estimation in the wild. *arXiv preprint arXiv:2108.12617*, 2021.

- [73] Qitao Zhao, Ce Zheng, Mengyuan Liu, and Chen Chen. A single 2d pose with context is worth hundreds for 3d human pose estimation. *Advances in Neural Information Processing Systems*, 36:27394–27413, 2023.
- [74] Silvia Zuffi, Angjoo Kanazawa, David W Jacobs, and Michael J Black. 3d menagerie: Modeling the 3d shape and pose of animals. In *Proceedings of the IEEE conference on computer vision and pattern recognition*, pages 6365–6373, 2017.
- [75] Silvia Zuffi, Angjoo Kanazawa, and Michael J. Black. Lions and tigers and bears: Capturing non-rigid, 3D, articulated shape from images. In *IEEE Conference on Computer Vision and Pattern Recognition (CVPR)*, pages 3955–3963. IEEE Computer Society, 2018.
- [76] Silvia Zuffi, Angjoo Kanazawa, Tanya Berger-Wolf, and Michael J. Black. Three-d safari: Learning to estimate zebra pose, shape, and texture from images "in the wild". In *International Conference on Computer Vision*, 2019.
- [77] Silvia Zuffi, Ylva Mellbin, Ci Li, Markus Hoeschle, Hedvig Kjellstrom, Senya Polikovsky, Elin Hernlund, and Michael J. Black. Varen: Very accurate and realistic equine network. In *2024 IEEE/CVF Conference on Computer Vision and Pattern Recognition (CVPR)*, pages 5374–5383, 2024.

NeurIPS Paper Checklist

1. Claims

Question: Do the main claims made in the abstract and introduction accurately reflect the paper's contributions and scope?

Answer: [\[Yes\]](#)

Justification: Each of our main claims including automated pipeline, curated benchmark, evaluation of existing methods and improved baseline are directly discussed in Section [3](#) and Section [4](#).

Guidelines:

- The answer NA means that the abstract and introduction do not include the claims made in the paper.
- The abstract and/or introduction should clearly state the claims made, including the contributions made in the paper and important assumptions and limitations. A No or NA answer to this question will not be perceived well by the reviewers.
- The claims made should match theoretical and experimental results, and reflect how much the results can be expected to generalize to other settings.
- It is fine to include aspirational goals as motivation as long as it is clear that these goals are not attained by the paper.

2. Limitations

Question: Does the paper discuss the limitations of the work performed by the authors?

Answer: [\[Yes\]](#)

Justification: Limitations are discussed in main paper Limitations section.

Guidelines:

- The answer NA means that the paper has no limitation while the answer No means that the paper has limitations, but those are not discussed in the paper.
- The authors are encouraged to create a separate "Limitations" section in their paper.
- The paper should point out any strong assumptions and how robust the results are to violations of these assumptions (e.g., independence assumptions, noiseless settings, model well-specification, asymptotic approximations only holding locally). The authors should reflect on how these assumptions might be violated in practice and what the implications would be.
- The authors should reflect on the scope of the claims made, e.g., if the approach was only tested on a few datasets or with a few runs. In general, empirical results often depend on implicit assumptions, which should be articulated.
- The authors should reflect on the factors that influence the performance of the approach. For example, a facial recognition algorithm may perform poorly when image resolution is low or images are taken in low lighting. Or a speech-to-text system might not be used reliably to provide closed captions for online lectures because it fails to handle technical jargon.
- The authors should discuss the computational efficiency of the proposed algorithms and how they scale with dataset size.
- If applicable, the authors should discuss possible limitations of their approach to address problems of privacy and fairness.
- While the authors might fear that complete honesty about limitations might be used by reviewers as grounds for rejection, a worse outcome might be that reviewers discover limitations that aren't acknowledged in the paper. The authors should use their best judgment and recognize that individual actions in favor of transparency play an important role in developing norms that preserve the integrity of the community. Reviewers will be specifically instructed to not penalize honesty concerning limitations.

3. Theory assumptions and proofs

Question: For each theoretical result, does the paper provide the full set of assumptions and a complete (and correct) proof?

Answer: [NA]

Justification: The paper does not include theoretical results.

Guidelines:

- The answer NA means that the paper does not include theoretical results.
- All the theorems, formulas, and proofs in the paper should be numbered and cross-referenced.
- All assumptions should be clearly stated or referenced in the statement of any theorems.
- The proofs can either appear in the main paper or the supplemental material, but if they appear in the supplemental material, the authors are encouraged to provide a short proof sketch to provide intuition.
- Inversely, any informal proof provided in the core of the paper should be complemented by formal proofs provided in appendix or supplemental material.
- Theorems and Lemmas that the proof relies upon should be properly referenced.

4. Experimental result reproducibility

Question: Does the paper fully disclose all the information needed to reproduce the main experimental results of the paper to the extent that it affects the main claims and/or conclusions of the paper (regardless of whether the code and data are provided or not)?

Answer: [Yes]

Justification: All experiments results are reproducible using the submitted code and dataset.

Guidelines:

- The answer NA means that the paper does not include experiments.
- If the paper includes experiments, a No answer to this question will not be perceived well by the reviewers: Making the paper reproducible is important, regardless of whether the code and data are provided or not.
- If the contribution is a dataset and/or model, the authors should describe the steps taken to make their results reproducible or verifiable.
- Depending on the contribution, reproducibility can be accomplished in various ways. For example, if the contribution is a novel architecture, describing the architecture fully might suffice, or if the contribution is a specific model and empirical evaluation, it may be necessary to either make it possible for others to replicate the model with the same dataset, or provide access to the model. In general, releasing code and data is often one good way to accomplish this, but reproducibility can also be provided via detailed instructions for how to replicate the results, access to a hosted model (e.g., in the case of a large language model), releasing of a model checkpoint, or other means that are appropriate to the research performed.
- While NeurIPS does not require releasing code, the conference does require all submissions to provide some reasonable avenue for reproducibility, which may depend on the nature of the contribution. For example
 - (a) If the contribution is primarily a new algorithm, the paper should make it clear how to reproduce that algorithm.
 - (b) If the contribution is primarily a new model architecture, the paper should describe the architecture clearly and fully.
 - (c) If the contribution is a new model (e.g., a large language model), then there should either be a way to access this model for reproducing the results or a way to reproduce the model (e.g., with an open-source dataset or instructions for how to construct the dataset).
 - (d) We recognize that reproducibility may be tricky in some cases, in which case authors are welcome to describe the particular way they provide for reproducibility. In the case of closed-source models, it may be that access to the model is limited in some way (e.g., to registered users), but it should be possible for other researchers to have some path to reproducing or verifying the results.

5. Open access to data and code

Question: Does the paper provide open access to the data and code, with sufficient instructions to faithfully reproduce the main experimental results, as described in supplemental material?

Answer: [\[Yes\]](#)

Justification: The code is publicly available. Due to licensing concerns around redistributing RGB video frames from YouTube, the dataset is currently provided via a private preview link for review purposes only. In the public release, we will exclude raw RGB frames and instead provide all processed annotations (e.g., keypoints, masks, depth maps) along with scripts and instructions for users to recover the necessary data locally. This approach ensures legal compliance while still supporting reproducibility.

Guidelines:

- The answer NA means that paper does not include experiments requiring code.
- Please see the NeurIPS code and data submission guidelines (<https://nips.cc/public/guides/CodeSubmissionPolicy>) for more details.
- While we encourage the release of code and data, we understand that this might not be possible, so “No” is an acceptable answer. Papers cannot be rejected simply for not including code, unless this is central to the contribution (e.g., for a new open-source benchmark).
- The instructions should contain the exact command and environment needed to run to reproduce the results. See the NeurIPS code and data submission guidelines (<https://nips.cc/public/guides/CodeSubmissionPolicy>) for more details.
- The authors should provide instructions on data access and preparation, including how to access the raw data, preprocessed data, intermediate data, and generated data, etc.
- The authors should provide scripts to reproduce all experimental results for the new proposed method and baselines. If only a subset of experiments are reproducible, they should state which ones are omitted from the script and why.
- At submission time, to preserve anonymity, the authors should release anonymized versions (if applicable).
- Providing as much information as possible in supplemental material (appended to the paper) is recommended, but including URLs to data and code is permitted.

6. Experimental setting/details

Question: Does the paper specify all the training and test details (e.g., data splits, hyper-parameters, how they were chosen, type of optimizer, etc.) necessary to understand the results?

Answer: [\[Yes\]](#)

Justification: We discuss necessary details in the supplementary sections. Other details follows the setting of [\[35\]](#).

Guidelines:

- The answer NA means that the paper does not include experiments.
- The experimental setting should be presented in the core of the paper to a level of detail that is necessary to appreciate the results and make sense of them.
- The full details can be provided either with the code, in appendix, or as supplemental material.

7. Experiment statistical significance

Question: Does the paper report error bars suitably and correctly defined or other appropriate information about the statistical significance of the experiments?

Answer: [\[No\]](#)

Justification: Running inference and evaluation is computationally expensive due to optimization on each single instance, making statistical significance analysis impractical in typical academic settings.

Guidelines:

- The answer NA means that the paper does not include experiments.

- The authors should answer "Yes" if the results are accompanied by error bars, confidence intervals, or statistical significance tests, at least for the experiments that support the main claims of the paper.
- The factors of variability that the error bars are capturing should be clearly stated (for example, train/test split, initialization, random drawing of some parameter, or overall run with given experimental conditions).
- The method for calculating the error bars should be explained (closed form formula, call to a library function, bootstrap, etc.)
- The assumptions made should be given (e.g., Normally distributed errors).
- It should be clear whether the error bar is the standard deviation or the standard error of the mean.
- It is OK to report 1-sigma error bars, but one should state it. The authors should preferably report a 2-sigma error bar than state that they have a 96% CI, if the hypothesis of Normality of errors is not verified.
- For asymmetric distributions, the authors should be careful not to show in tables or figures symmetric error bars that would yield results that are out of range (e.g. negative error rates).
- If error bars are reported in tables or plots, The authors should explain in the text how they were calculated and reference the corresponding figures or tables in the text.

8. Experiments compute resources

Question: For each experiment, does the paper provide sufficient information on the computer resources (type of compute workers, memory, time of execution) needed to reproduce the experiments?

Answer: **[Yes]**

Justification: We discuss necessary details in the supplementary sections. Other details follows the setting of [35].

Guidelines:

- The answer NA means that the paper does not include experiments.
- The paper should indicate the type of compute workers CPU or GPU, internal cluster, or cloud provider, including relevant memory and storage.
- The paper should provide the amount of compute required for each of the individual experimental runs as well as estimate the total compute.
- The paper should disclose whether the full research project required more compute than the experiments reported in the paper (e.g., preliminary or failed experiments that didn't make it into the paper).

9. Code of ethics

Question: Does the research conducted in the paper conform, in every respect, with the NeurIPS Code of Ethics <https://neurips.cc/public/EthicsGuidelines>?

Answer: **[Yes]**

Justification: We collect data from publicly available data in accordance with platform terms, and avoid redistributing raw video content directly to respect copyright and privacy. We plan to release only derived annotations along with tools to regenerate necessary data locally. No personally identifiable information or real animal is involved in this work.

Guidelines:

- The answer NA means that the authors have not reviewed the NeurIPS Code of Ethics.
- If the authors answer No, they should explain the special circumstances that require a deviation from the Code of Ethics.
- The authors should make sure to preserve anonymity (e.g., if there is a special consideration due to laws or regulations in their jurisdiction).

10. Broader impacts

Question: Does the paper discuss both potential positive societal impacts and negative societal impacts of the work performed?

Answer: [Yes]

Justification: As described in the introduction, our work aims to advance non-invasive research on animal motion and behavior. We also acknowledge the potential copyright and privacy concerns associated with releasing raw video data, which we discuss further in the supplementary material. To address these concerns, we publicly release only the derived annotations and processed data, excluding the original RGB video frames.

Guidelines:

- The answer NA means that there is no societal impact of the work performed.
- If the authors answer NA or No, they should explain why their work has no societal impact or why the paper does not address societal impact.
- Examples of negative societal impacts include potential malicious or unintended uses (e.g., disinformation, generating fake profiles, surveillance), fairness considerations (e.g., deployment of technologies that could make decisions that unfairly impact specific groups), privacy considerations, and security considerations.
- The conference expects that many papers will be foundational research and not tied to particular applications, let alone deployments. However, if there is a direct path to any negative applications, the authors should point it out. For example, it is legitimate to point out that an improvement in the quality of generative models could be used to generate deepfakes for disinformation. On the other hand, it is not needed to point out that a generic algorithm for optimizing neural networks could enable people to train models that generate Deepfakes faster.
- The authors should consider possible harms that could arise when the technology is being used as intended and functioning correctly, harms that could arise when the technology is being used as intended but gives incorrect results, and harms following from (intentional or unintentional) misuse of the technology.
- If there are negative societal impacts, the authors could also discuss possible mitigation strategies (e.g., gated release of models, providing defenses in addition to attacks, mechanisms for monitoring misuse, mechanisms to monitor how a system learns from feedback over time, improving the efficiency and accessibility of ML).

11. Safeguards

Question: Does the paper describe safeguards that have been put in place for responsible release of data or models that have a high risk for misuse (e.g., pretrained language models, image generators, or scraped datasets)?

Answer: [Yes]

Justification: In supplementary, we discuss the copyright considerations and the potential for unintended privacy issues. We release only the derived data without original RGB frames.

Guidelines:

- The answer NA means that the paper poses no such risks.
- Released models that have a high risk for misuse or dual-use should be released with necessary safeguards to allow for controlled use of the model, for example by requiring that users adhere to usage guidelines or restrictions to access the model or implementing safety filters.
- Datasets that have been scraped from the Internet could pose safety risks. The authors should describe how they avoided releasing unsafe images.
- We recognize that providing effective safeguards is challenging, and many papers do not require this, but we encourage authors to take this into account and make a best faith effort.

12. Licenses for existing assets

Question: Are the creators or original owners of assets (e.g., code, data, models), used in the paper, properly credited and are the license and terms of use explicitly mentioned and properly respected?

Answer: [Yes]

Justification: We properly cite all methods and models used in our data pipeline and experiments.

Guidelines:

- The answer NA means that the paper does not use existing assets.
- The authors should cite the original paper that produced the code package or dataset.
- The authors should state which version of the asset is used and, if possible, include a URL.
- The name of the license (e.g., CC-BY 4.0) should be included for each asset.
- For scraped data from a particular source (e.g., website), the copyright and terms of service of that source should be provided.
- If assets are released, the license, copyright information, and terms of use in the package should be provided. For popular datasets, paperswithcode.com/datasets has curated licenses for some datasets. Their licensing guide can help determine the license of a dataset.
- For existing datasets that are re-packaged, both the original license and the license of the derived asset (if it has changed) should be provided.
- If this information is not available online, the authors are encouraged to reach out to the asset's creators.

13. New assets

Question: Are new assets introduced in the paper well documented and is the documentation provided alongside the assets?

Answer: [Yes]

Justification: We provide code and dataset along with instructions of running the code and dataset specifications.

Guidelines:

- The answer NA means that the paper does not release new assets.
- Researchers should communicate the details of the dataset/code/model as part of their submissions via structured templates. This includes details about training, license, limitations, etc.
- The paper should discuss whether and how consent was obtained from people whose asset is used.
- At submission time, remember to anonymize your assets (if applicable). You can either create an anonymized URL or include an anonymized zip file.

14. Crowdsourcing and research with human subjects

Question: For crowdsourcing experiments and research with human subjects, does the paper include the full text of instructions given to participants and screenshots, if applicable, as well as details about compensation (if any)?

Answer: [NA]

Justification: This work does not involve crowdsourcing nor research with human subjects.

Guidelines:

- The answer NA means that the paper does not involve crowdsourcing nor research with human subjects.
- Including this information in the supplemental material is fine, but if the main contribution of the paper involves human subjects, then as much detail as possible should be included in the main paper.
- According to the NeurIPS Code of Ethics, workers involved in data collection, curation, or other labor should be paid at least the minimum wage in the country of the data collector.

15. Institutional review board (IRB) approvals or equivalent for research with human subjects

Question: Does the paper describe potential risks incurred by study participants, whether such risks were disclosed to the subjects, and whether Institutional Review Board (IRB) approvals (or an equivalent approval/review based on the requirements of your country or institution) were obtained?

Answer: [NA]

Justification: This work does not involve crowdsourcing nor research with human subjects.

Guidelines:

- The answer NA means that the paper does not involve crowdsourcing nor research with human subjects.
- Depending on the country in which research is conducted, IRB approval (or equivalent) may be required for any human subjects research. If you obtained IRB approval, you should clearly state this in the paper.
- We recognize that the procedures for this may vary significantly between institutions and locations, and we expect authors to adhere to the NeurIPS Code of Ethics and the guidelines for their institution.
- For initial submissions, do not include any information that would break anonymity (if applicable), such as the institution conducting the review.

16. Declaration of LLM usage

Question: Does the paper describe the usage of LLMs if it is an important, original, or non-standard component of the core methods in this research? Note that if the LLM is used only for writing, editing, or formatting purposes and does not impact the core methodology, scientific rigorousness, or originality of the research, declaration is not required.

Answer: [Yes]

Justification: We describe the role of LLM in our data pipeline and provide the prompts we use in supplementary materials.

Guidelines:

- The answer NA means that the core method development in this research does not involve LLMs as any important, original, or non-standard components.
- Please refer to our LLM policy (<https://neurips.cc/Conferences/2025/LLM>) for what should or should not be described.

Appendix

A Data Pipeline Implementation Detail

A.1 Database

We incorporate SQLite, a lightweight local file-based database system, to store metadata generated during processing and enable parallel execution of multiple processes across the same or different stages. Specifically, each intermediate result after Stage 1 and Stage 2 contains a status field that records whether a video or clip is unprocessed, being processed, completed, or discarded. These statuses are dynamically checked and updated by the processing pipeline, ensuring efficient parallel execution on large-scale data. Additionally, we store metadata such as video titles, query phrases, and keywords, which may facilitate the development of multimodal animal motion studies, such as motion retrieval and generation.

A.2 Video Scraping

We leverage GPT for automatic search query generation. To make search queries as diverse as possible, we first ask GPT to generate a set of more specific sub-category breeds, for example, *Clydesdale* and *Mustang*. Separately, GPT is asked to generate a set of context phrases that are related to the category of interests, for instance, *racing competition* and *in a farm* for horse. Finally, we randomly combine two sets to form a list of diverse search texts to query YouTube for raw videos. Specifically, given a category name of an animal, we use the following prompt to generate diverse sub-category or breed, where n is set to 10, and *category* is the name of category of interests, e.g. *horse*:

List $\{n\}$ types of $\{\text{category}\}$. Only show the list in python list format without using a code block.

Similarly, we generate query phrases with the following prompt, with n set to 10 as well:

*List $\{n\}$ search phrases or autocompletions for searching $\{\text{category}\}$ videos on a video sharing website. Assume user already input the word *category*, only show the trailing phrases. Only show the list in python list format without using a code block.*

We then combine them in a set-product manner to generate search queries for YouTube.

Since the YouTube API imposes rate and usage limits, we employ a web automation framework to simulate human searches via a web browser, which bypasses these restrictions.

After this stage, each downloaded video is stored in the database with a unique YouTube video ID.

Our downloading pipeline is implemented based on Selenium Webdriver [5] for querying and retrieving video ID results and pytube [10] for downloading the videos.

A.3 Preprocessing

This stage preprocesses raw videos for object tracking, aiming to create animal-centric crops. Raw videos are filtered to remove frames lacking the target animal.

At this stage, downloaded videos are first retrieved from the database. The videos are then cut into clips based on shot changes using pycenedetect [13].

Specifically, we compute the average pixel difference between consecutive frames in the HSV color space and set a threshold of 25 to determine shot boundaries. Clips shorter than 30 frames are discarded. While this algorithm is effective in most cases, it fails to detect fading effects, which we address in Stage 3. Using a similar pixel-difference-based approach, we also remove clips consisting solely of still frames with no pixel changes. Additionally, we compute an average CLIPScore for each clip by randomly sampling 10 frames and comparing them against the prompt: "A photo of category." All video clips are downsampled to 10 frames per second to enhance processing efficiency in later

stages. Similar to the first stage, the status of the source video and processed clips is dynamically monitored and updated throughout this process.

A.4 Tracking

At this stage, processed clips are retrieved from the database, and tracking with segmentation is performed.

Specifically, we apply grounding results on the first frame as a visual prompt to SAM, then track for 50 consecutive frames. This process is iterated for the next 50 frames, using location-based association to link tracks between the end of the current interval and the beginning of the next.

This enables long-term tracking while also allowing the detection and tracking of newly appearing objects.

After obtaining the initial tracking results with segmentation, we sequentially apply the filtering steps.

Overlapping Instances. When multiple animals are present in a frame, off-the-shelf keypoint estimators may become confused and incorrectly assign keypoints to different instances, especially when significant overlap occurs. To mitigate this, we remove frames from tracks where two or more animals overlap substantially. We achieve this by thresholding the Intersection over Union (IoU) between each pair of animals in the same frame and removing both mask silhouettes from the tracks if their IoU exceeds the threshold.

Low Resolution Instances. If the animal is too small in the frame, subsequent operations such as keypoints and feature extraction may have degraded performance due to low resolution after resizing. Therefore we discard any frames from the track where the bounding box area of the animal is less than 1/4 of the final crop size, *e.g.* 256×256 if the final crop size is 512×512 .

Truncated Instances. In many cases, an animal’s full body is not visible within the video frame. Since animal reconstruction methods rely on mask silhouettes as shape supervision, truncated silhouettes can lead to inaccurate reconstructions with unnatural poses and shapes. We remove frames from the tracks if the bounding box is too close to the frame border, as these typically indicate a truncated animal.

Inconsistent Tracks. Tracking algorithms may fail when videos contain ambiguous cases or unnatural artifacts. A common failure occurs when multiple animals with similar appearances are present, causing the algorithm to switch identities and track different animals inconsistently. Another failure case arises from video fading effects, which are difficult to detect using shot detection algorithms in earlier stages. In some instances, the tracking algorithm may fail to stop even after a shot change or fade-out, continuing to track a different object or background in the new shot. To mitigate these issues, we apply a threshold on the bounding box IoU between adjacent frames of the same track and remove all frames following a detected low IoU.

Temporal Postprocessing. At this stage, some unqualified frames have been filtered from the tracking results, creating discontinuities. To address this, we apply a post-processing step based on predefined parameters for minimal track length, maximal track length, and the allowed gap within a track. By iterating through all frames in a track, we identify gaps exceeding the allowed threshold or instances where the track reaches the maximal length; in such cases, the subsequent frames are split into a new track. If a gap falls within the allowed threshold, we resegment missing mask silhouette using SAM-2, interpolating bounding boxes from both sides as input prompts. Any tracks shorter than the minimal track length are discarded.

Object-centric Cropping. To obtain the final object-centric video crops for animal reconstruction, we generate square crop boxes centered on the bounding box of the animal in each frame. The size of each crop box is determined by a predefined ratio relative to the mask area. We further apply moving average smoothing to the crop boxes before cropping and resizing all frames to a standardized size. As a final filtering step, we randomly select a cropped RGB image for each track and input it into GPT to identify and remove instances of false detection or heavily occluded animals.

To determine the crop box for each frame in the track, we align the centers of the bounding box and crop box, then extract a square with an area equal to $2 \times$ the bounding box area.

We smooth the crop box centers using a moving average with a window size of 10 frames to reduce jitter in the tracking results. Finally, we apply gpt-4o-mini to filter tracks using one sampled frame from each track with the prompt:

Does this image show a realistic photo of a {category} without any occlusion? Answer yes or no only.

A.5 Features and Auxiliaries Processing

Immediately after each track is saved, we post-process the cropped tracks to generate auxiliary data. Specifically, we integrate ViTPose++ [63] for animal keypoints estimation, DINOv2 [43] for image feature, SEA-RAFT [59] for optical flow estimation, and Depth Anything V2 [67] for depth estimation. For occlusion boundary, we extract depth values at the dilated and eroded mask boundaries, respectively. Then for each pixel on the original mask boundary, we calculate the depth difference between the nearest pixel on the dilated boundary and the nearest pixel on the eroded boundary. This depth difference helps determine whether the pixels outside the animal silhouette belong to the foreground, indicating occlusion, or the background, indicating no occlusion at that region. At this stage, all tracks are stored in the database with computed mean occlusion and optical flow values. If needed, users can further filter the data based on occlusion proportion and optical flow thresholds.

B Details of Benchmark

B.1 Task Formulation

Similar to the 3D animal reconstruction task, which aims to estimate an animal’s 3D pose and shape from a single image, the 4D animal reconstruction task seeks to estimate a sequence of 3D poses and shapes from a sequence of frames of the same animal. Beside RGB image input, typical methods also require other 2D auxiliary data as guidance, such as mask silhouettes and 2D keypoints, obtained either from manual labeling or from pretrained vision models. Formally, given an RGB video input $\mathcal{V}_T = \{v_t\}_{t=1}^T \in \mathbb{R}^{T \times 3 \times H \times W}$ of an animal, along with any required auxiliary input $\mathcal{A}_T = \{a_t\}_{t=1}^T$, in $\{0, 1\}^{T \times H \times W}$ in the case of 2D mask or in $\mathbb{R}^{T \times K \times 2}$ in the case of 2D keypoints for instance, a function $f_\theta : \{\mathcal{V}, \mathcal{A}\} \mapsto \mathcal{S}$ is expected to output a sequence of posed 3D shapes $\mathcal{S}_T = \{s_t\}_{t=1}^T$ that naturally resembles the shape and pose sequence shown in the input video \mathcal{V}_T , where T is number of frames in sequence, H and W are spatial dimensions of the frames, K is number of defined keypoints. Function f_θ can operate either as a feed-forward model using pretrained parameter θ , or by optimizing θ at test time. Since different methods operate differently—some requiring large-scale training data [35] while others only perform test-time optimization [74, 7]—our benchmark dataset is designed for evaluation only to ensure fair comparisons.

B.2 Metrics

Silhouette Intersection-over-union (IoU). We follow previous works [9, 76, 4, 58, 49, 69] to employ silhouette intersection-over-union (IoU). Silhouette IoU measures the IoU between the ground truth silhouette mask and the silhouette mask rendered by the reconstructed 3D shape. Although a high 2D IoU does not necessarily correspond to a natural 3D shape due to potential ambiguities, a low IoU reliably indicates that the reconstruction is underperforming.

Percentage of Correct Keypoint (PCK). Following previous works [24, 33, 30, 60, 61, 35], we use the Percentage of Correct Keypoints (PCK) metric, which measures the percentage of projected keypoints that fall within a fixed multiple of a normalizing distance threshold. Studies have defined different distance thresholds. Following [9, 31, 8], we use the square root of the ground-truth mask silhouette area as the normalizing distance threshold.

Keypoint Transfer (KT). Since no ground-truth 3D keypoint or shape annotations exist, previous works [61, 35, 29, 30, 69, 33, 8, 28] use Keypoint Transfer (KT) as a proxy for evaluating reconstructed 3D shapes. Specifically, a set of ground-truth 2D keypoints from a source image is projected onto the reconstructed 3D shape surface to establish a mapping with surface vertices. The corresponding vertices are then reprojected from the 3D shape onto a target image with novel view and pose. PCK is computed using the reprojected keypoints and the ground-truth keypoints in the target image. A well-reconstructed 3D shape should exhibit consistency, producing low errors after undergoing this 2D-to-3D-to-2D mapping.

Mean Per-Joint Velocity Error (MPJVE). As our work is the first to specifically address the task of 4D animal reconstruction, there are no established metrics for evaluating temporal aspects such as motion smoothness or consistency over time in animal domain. Following related works in human motion estimation [44, 54, 73], we adopt Mean Per-Joint Velocity Error (MPJVE) to quantify the discrepancy in joint velocity within the projected, normalized pixel space. Specifically, for each joint across two consecutive frames, we compute the magnitude of the vector difference between the ground-truth velocity and the predicted velocity. The final MPJVE is obtained by averaging the error over all joints and all frames.

C 4D-Fauna Implementation Detail

Preliminary. 3D-Fauna builds upon MagicPony [61], which learns a prior shape for a specific animal category from diverse images of that category by leveraging self-supervised DINO-ViT [12] features. It then applies instance-specific predicted parameters, such as deformation and articulation, for inverse rendering supervision. Building on this, 3D-Fauna introduces a learnable prior shape bank, which functions as a dictionary of features capable of dynamically combining basis shapes during training and inference to generate diverse instance-specific prior 3D shapes. As a result, 3D-Fauna removes the constraint of training and inference on a single category, enabling it to learn a rich prior shape bank from pan-category images and produce diverse prior shapes at inference time.

C.1 Canonical Shape Prediction

We use the pretrained 3D-Fauna model as initialization and optimize only the deformation predictor along with the newly introduced per-frame camera and articulation parameters. Given a sequence of video frame input \mathcal{V}_T , the frozen image encoder will return a sequence of image features ϕ_T . To ensure a consistent shape across different frames, we compute a mean feature $\bar{\phi} = \frac{1}{T} \sum_{t=1}^T \phi_t$, used for predict a prior shape for all frames. We also use the mean feature to input the deformation predictor, guiding it to learn a consistent deformation field that better fit the shape to the masks of the sequence. Specifically, a prior shape predictor f_{prior} will predict a mesh $(V, F) = f_{\text{prior}}(\bar{\phi})$, where V and F are mesh vertices and faces, and a deformation predictor f_{deform} will predict a deformation $\Delta V = f_{\text{deform}}(V, \bar{\phi})$, resulting in a canonical shape $(V + \Delta V, F)$.

C.2 Per Frame Pose Prediction

The inaccurate reconstruction results from 3D-Fauna stem from the fact that its original predictor networks for camera pose and animal articulation are trained on diverse data, making them generalizable but not precise enough for individual instances. To refine the camera pose and animal articulation for a single sequence, we introduce per-frame parameters that are directly optimized, rather than fine-tuning the predictor networks. The outputs from the pretrained networks serve as initialization for this process. Specifically, we introduce per-frame articulation parameters $\{\xi_t\}_{t=1}^T$ and camera pose parameters $\{R_t\}_{t=1}^T$. For initialization, $\xi_t = f_{\text{art}}(\phi_t)$ and $R_t = f_{\text{cam}}(\phi_t)$, where f_{art} and f_{cam} are pretrained articulation and camera pose predictors, respectively. The canonical shape is first applied with per-frame articulation parameters, following a predefined kinematic tree and skinning function, to transform it into a posed shape. Together with the optimized camera pose parameters and a pretrained texture predictor, the final shape is rendered into an image, mask, and projected keypoints for direct supervision.

C.3 Keypoints supervision

Since the joints are defined differently between 3D-Fauna framework and output from off-the-shelf keypoint predictor, we identify joints with overlapping defining s for supervision. Specifically, we align node, tail base, and the bottom two joints on four legs, totaling 10 keypoints to calculate keypoint reprojection loss:

$$\mathcal{L}_{\text{kp}} = \|J - \hat{J}\|_2^2 \quad (1)$$

where $J \in \mathbb{R}^{10 \times 2}$ is the ground truth 2D keypoint and $\hat{J} \in \mathbb{R}^{10 \times 2}$ is the predicted keypoints projected onto 2D.

C.4 Temporal Smoothness Loss

We apply smoothness constraints on articulation angles, posed bones, and camera pose within a batch of frames. Specifically, we minimize both the difference of parameter values between consecutive frames and the difference of changes between consecutive intervals. For smoothness loss on articulation parameter:

$$\mathcal{R}_{\text{smooth,art}} = \sum_{t=1}^{T-1} \|\xi_{t+1} - \xi_t\|_2^2 + \sum_{t=1}^{T-2} \|(\xi_{t+2} - \xi_{t+1}) - (\xi_{t+1} - \xi_t)\|_2^2 \quad (2)$$

The losses are same for posed bone 3D coordinate and camera pose parameters, and overall:

$$\mathcal{R}_{\text{smooth}} = \mathcal{R}_{\text{smooth,art}} + \mathcal{R}_{\text{smooth,bone}} + \mathcal{R}_{\text{smooth,cam}} \quad (3)$$

C.5 Training Objective

The training objective is essentially the training objective of 3D-Fauna plus the newly added supervisions. From 3D-Fauna:

$$\mathcal{L}_{\text{3D-Fauna}} = \mathcal{L}_{\text{rec}} + \lambda_{\text{hyp}} \mathcal{L}_{\text{hyp}} + \lambda_{\text{adv}} \mathcal{L}_{\text{adv}} + \mathcal{R} \quad (4)$$

where,

$$\mathcal{L}_{\text{rec}} = \lambda_{\text{m}} \mathcal{L}_{\text{m}} + \lambda_{\text{im}} \mathcal{L}_{\text{im}} + \lambda_{\text{feat}} \mathcal{L}_{\text{feat}} \quad (5)$$

and

$$\mathcal{R} = \lambda_{\text{Eik}} \mathcal{R}_{\text{Eik}} + \lambda_{\text{art}} \mathcal{R}_{\text{art}} + \lambda_{\text{def}} \mathcal{R}_{\text{def}} \quad (6)$$

where \mathcal{L}_{m} is mask reconstruction loss, \mathcal{L}_{im} is image reconstruction loss, $\mathcal{L}_{\text{feat}}$ is feature reconstruction loss, \mathcal{L}_{hyp} is viewpoint hypothesis loss, \mathcal{L}_{adv} is mask shape adversarial loss, \mathcal{R}_{Eik} is the Eikonal constraint on SDF network for prior shape prediction, \mathcal{R}_{art} is regularization on articulation parameters, \mathcal{R}_{def} is regularization on deformations, and λ s are corresponding balancing loss weights. Adding the new loss terms:

$$\mathcal{L} = \mathcal{L}_{\text{3D-Fauna}} + \lambda_{\text{kp}} \mathcal{L}_{\text{kp}} + \lambda_{\text{kp}} \mathcal{R}_{\text{smooth}} \quad (7)$$

We set $\lambda_{\text{kp}} = \lambda_{\text{smooth}} = 50$. Since our prior shape is fixed, we set $\lambda_{\text{feat}} = \lambda_{\text{Eik}} = 0$. All other losses weights follow the implementation in 3D-Fauna.

C.6 Optimization

We use Adam optimizer with 0.1 learning rate. For each sequence, we construct data into batches of 8 consecutive frames in a sliding window manner. We optimize for 25 epochs for each sequence, starting from the pretrained 3D-Fauna model weights. We run on single L40 GPU with 48 GPU memory.

D Dataset Statistics

We show number of frames and number of videos per category of the collected full dataset in Figure 10

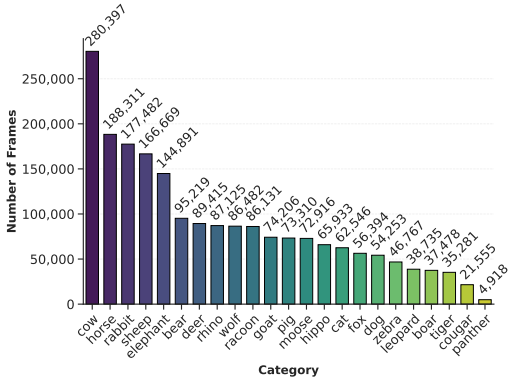


Figure 9: A detailed breakdown of the number of frames collected in full dataset for each animal category.

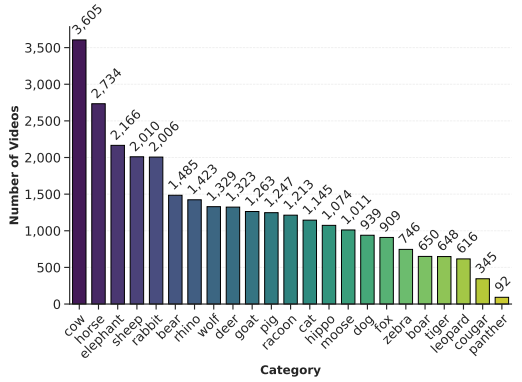


Figure 10: A detailed breakdown of the number of videos collected in full dataset for each animal category.

E Motion Type Analysis

We leverage Gemini [55] to annotate each motion video for further motion type analysis. Specifically, we choose a subset of 28 motion type labels defined in AnimalKingdom dataset [41] that are reasonable for quadrupeds. We use gemini-2.5-flash model and let it choose 1-3 motion type labels that best represent the given video. The statistics of the motion type is shown in

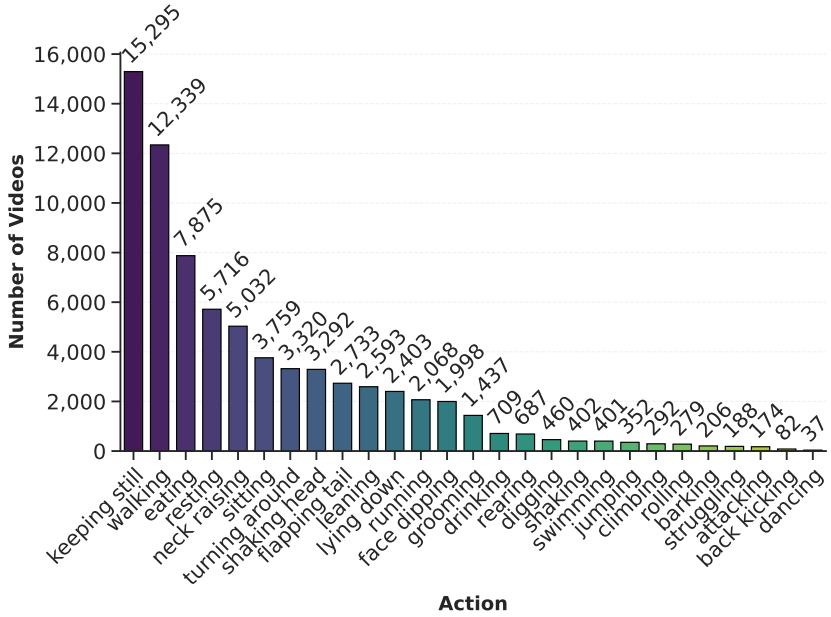


Figure 11: Distribution of motion types across the full dataset. Each video is assigned one to three labels.

F Visualization of Collected Data

We present a visualization of the video data collected using our proposed data pipeline, consisting of randomly sampled, uncurated object-centric videos with silhouettes applied. More sample data are included in the supplementary materials.



Figure 12: Visualization of random uncurated data collected by our data pipeline.

G Visualization of 4D Reconstruction Results

We show some additional visual results of 4D reconstruction results using different methods. Video results on sample data are included in supplementary materials.

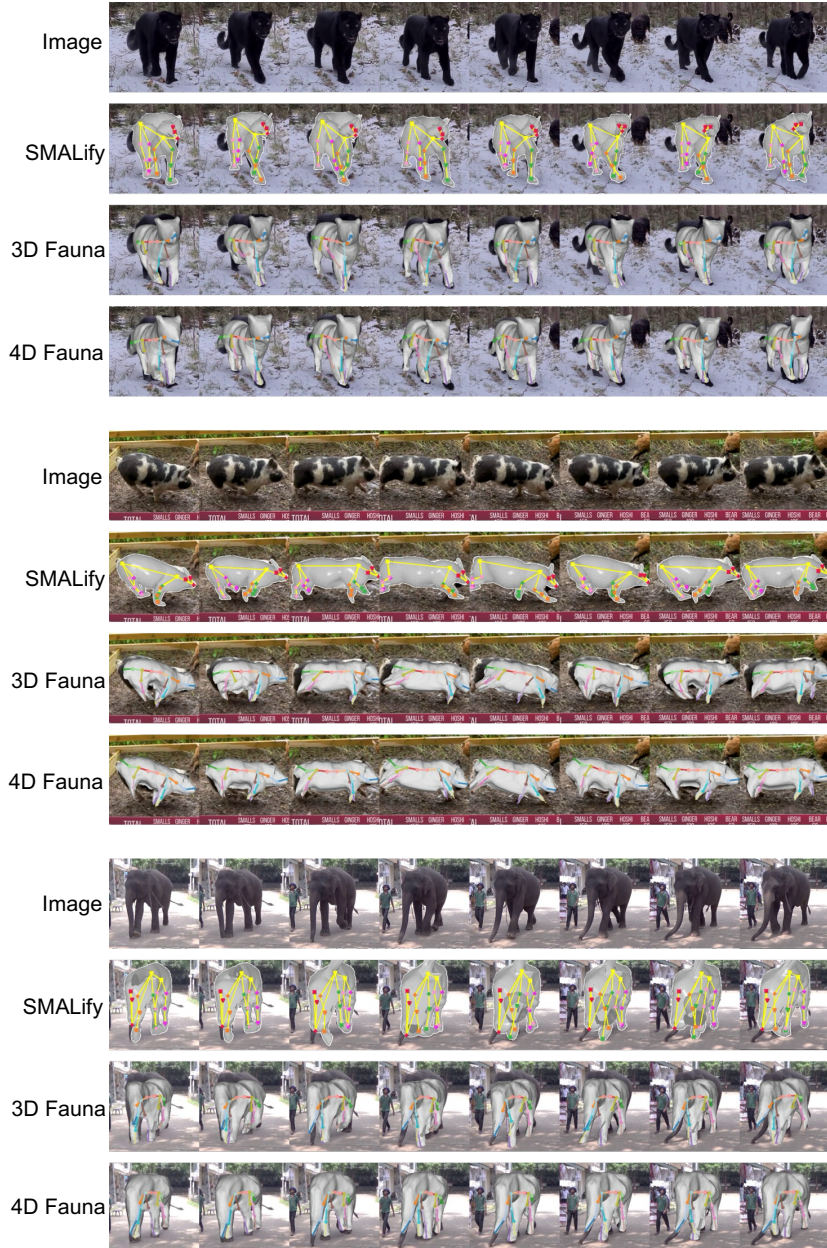


Figure 13: 4D reconstruction results comparison.

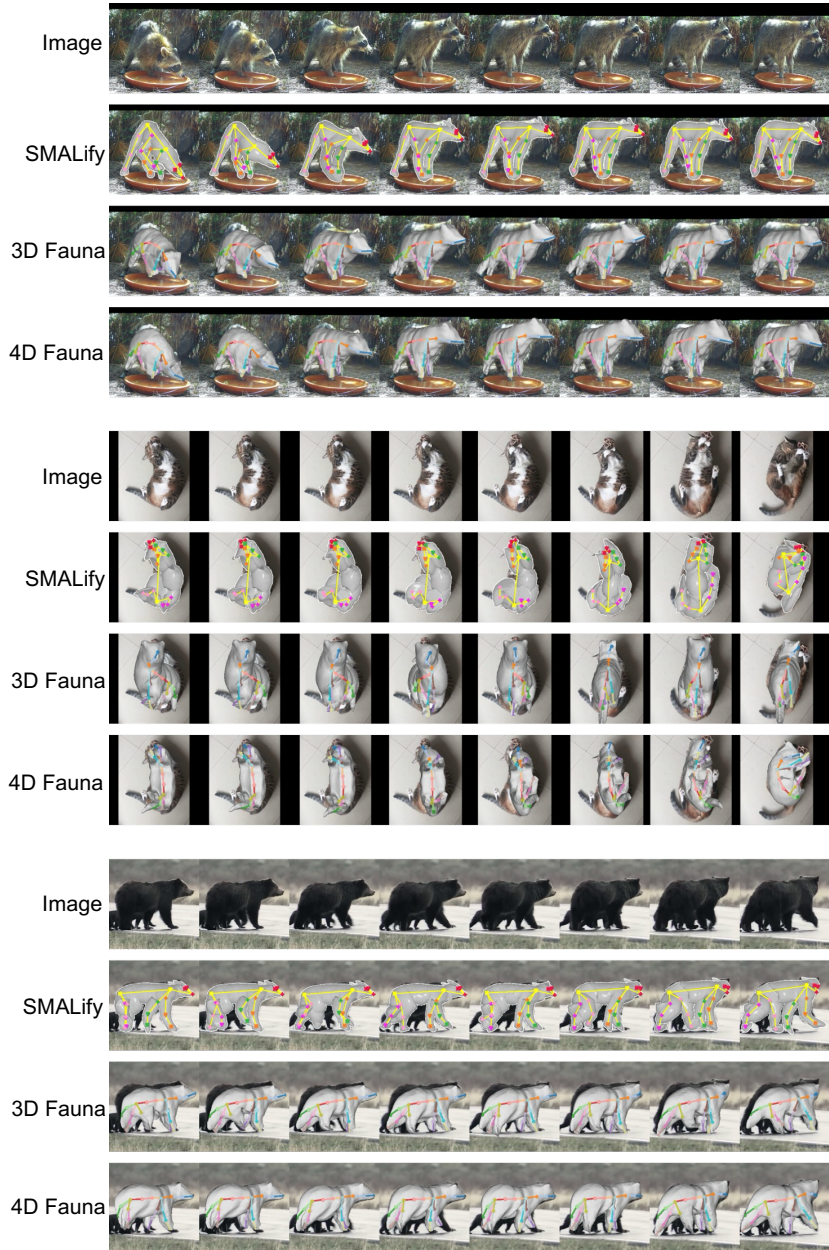


Figure 14: 4D reconstruction results comparison.